J Mater Sci (2007) 42:7882–7893
DOI 10.1007/s10853-007-1633-7

Influence of melt treatments on sliding wear behavior of Al–7Si and Al–7Si–2.5Cu cast alloys

K. G. Basavakumar · P. G. Mukunda · M. Chakraborty

Received: 16 October 2006 / Accepted: 20 February 2007 / Published online: 30 May 2007

Abstract The microstructures and dry sliding wear behavior of Al–7Si and Al–7Si–2.5Cu cast alloys were studied after various melt treatments like grain refinement and modification. Results indicate that combined grain refined and modified Al–7Si–2.5Cu cast alloys have microstructures consisting of uniformly distributed α-Al grains, eutectic Al– silicon and fine $CuAl_2$ particles in the interdendritic region. These alloys exhibited better wear resistance in the cast condition compared with the same alloy subjected to only grain refinement or modification. The improved wear resistances of Al–7Si–2.5Cu cast alloys are related to the refinement of the aluminum grain size, uniform distribution of eutectic Al-silicon and fine $CuAl_2$ particles in the interdendritic region resulting from combined refinement and modification. This paper attempts to investigate the influence of the microstructural changes in the Al–7Si and Al–7Si–2.5Cu cast alloys by grain refinement, modification and combined action of both on the sliding wear behavior.

Introduction

Some of the major driving forces for the development of Al–Si cast alloys are the superior wear resistance, low coefficient of thermal expansion (CTE), high corrosion resistance, high strength to weight ratio, excellent castability etc. which makes them potential candidate materials for a number of tribological applications in automobiles and other engineering sectors. The improvement in sliding wear resistance and mechanical properties is dictated by the type, shape, size and size distribution of second phase particles in the matrix and matrix microstructures. Hardness is usually thought of as a wear controlling property, i.e. the higher the hardness, more is the wear resistance of the material. However, it should be emphasized that it is the hardness of the contacting asperities and not the bulk hardness that will control the wear rate. The addition of hard second phase particles to the matrix improves both wear and mechanical properties [1–4]. In this sense, from a wear resistance point of view, it is interesting to minimize the occurrence of soft-hard contacts between sliding surfaces, which produce localized wear and would lead to premature failure. Microstructural tailoring allows optimizing the wear resistance, by obtaining a fine and homogeneous dispersion of α-Al grains and hard silicon particles.

In order to understand better the sliding wear mechanisms of metallic materials, a thorough analysis of their running-in (Break-in) behavior has been advocated [5]. It is during this initial stage in sliding that surface and their underlying microstructures are adjusting to the conditions, which may represent the major portion of their service lifetimes. Such adjustments frequently involve marked variations in friction coefficients and/or rates of wear. Many polyphase alloys are in use as wear resistant materials. If improvements in their performance are to be made, more needs to be known about the basic nature of their friction and wear mechanisms. Fundamental studies of metallurgical effects on sliding have largely involved pure metals and relatively simple single phase alloys. While much has been learned about the role of microstructure in

K. G. Basavakumar (✉) · P. G. Mukunda · M. Chakraborty
Department of Metallurgical and Materials Engineering, Indian Institute of Technology, Kharagpur 721302, India
e-mail: mbkumar29@rediffmail.com

such materials, additional basic research in tribology needs to be focused on the more complex, polyphase materials many of which are in wide use in service. One important class of these polyphase materials involves wear resistant microstructures in which hard particles are contained within a softer metal matrix.

Numerous studies have been reported on the wear behavior of Al–Si cast alloys. However, out of these reports it has been observed that, only a few have been devoted to investigating systematically the effect of second phase particles on tribological properties of aluminum and its alloys. While some authors report wear resistance is best in the hyper-eutectic [6], others report it to be in and around the eutectic [7], alternatively, some authors report that silicon has no effect on wear of Al–Si alloys until it exceeds 20 wt% [8–9]. Sarkar [10] studied the wear of Al–Si alloys against hardened steel disc and gray cast iron and reported that the hyper eutectic alloys wear more than the hypo eutectic alloys. Clarke et al. [7] conducted some experiments on a series of Al–Si alloys with varying silicon content up to 21 wt% and found that the wear resistance of Al–Si alloys improved with silicon content up to only near eutectic composition and the hyper eutectic alloys wear more than the hypo eutectic alloys. Somi reddy et al. [11] investigated the wear and seizure behavior of Al–Si alloys varying silicon content up to 23 wt% using Pin-On-Disc machine under a wide load range 15–200 N. It was observed that addition of silicon to aluminum improves wear and seizure resistance. It was suggested that seizure occurred at a definite temperature value. Eyre has also investigated microstructural effects on the wear of Al–Si alloys [12]. He found that varying the amount of copper and Fe in the alloy changes the load at which a transition from mild (Oxidative) wear to severe (Metallic) wear occurred. Earlier work by Shivanath [6] demonstrated that increasing the silicon content in Al–Si alloys linearly increased the transition load. The load at which the transition in wear mode occurred was also found to be affected by the choice of counter face material.

From the foregoing discussion, it is clear that many mechanisms can play a significant role in the sliding wear behavior of complex polyphase alloys. Many previous studies on the fundamental metallurgical mechanisms of friction and wear in pure metals and single phase alloys have provided a basis for interpreting their sliding wear behavior, but investigators only rarely have pursued the more rigorous questions involved with understanding the mechanistic details of sliding wear behavior of the complex microstructures typical of many grain refined and modified materials. If timely progress is to be made in this area, more tools of basic metals research need to be focused on the alloys of current technological significance. The aim of the present work is to investigate the influence of grain refiner and/or modifier and combined addition of both on sliding wear behavior of Al–7Si and Al–7Si–2.5Cu cast alloys in dry sliding against a steel counter face by using computerized Pin-On Disc wear tests.

Experimental details

Al–7Si alloy was prepared by melting commercially pure aluminum (99.7%) with Al–20 wt% Si master alloy in clay graphite crucible in a pit type resistance furnace under a cover flux (45%NaCl + 45% KCl + 10% NaF) and the melt was held at 720 °C. After degassing with 1% solid hexachloroethane, master alloy chips duly packed in aluminum foil were added to the melt for grain refinement. For modification Al–10 wt% Sr master alloy was used with addition level being kept constant at 0.02 wt% Sr [3]. The melt was stirred for 30 s after the addition of grain refiner and/or modifier. Melts were held for 5 min and poured into a cylindrical graphite mould surrounded by fireclay brick. The details of the alloys, grain refinement and modification treatment and mechanical properties of various alloys are given in Table 1. The chemical compositions of the cast alloys and master alloys assessed using atomic emission spectroscopy are given in Table 2. The microstructures of the samples that had been cut in the longitudinal direction were studied. Grain size analysis was carried out by the linear intercept method after etching the polished surface with Keller's reagent (2.5% HNO_3, 1.5% HCl, 1% HF and 95% H_2O). Samples for optical microscopy were electro polished using in an electrolytic bath comprising of 80% methanol and 20% HNO_3 by volume. Selected samples were subjected to SEM and XRD analysis.

The sliding wear tests were carried out using Pin-On-Disc tribometer [TR-20, DUCOM-PIN-ON-DISC]. Schematic diagram is shown in Fig. 1. The pins of 8-mm diameter and 25-mm length were fabricated from the castings against a hardened and ground (Ra = 0.1 μm) En-24 steel disc [Dia-100 mm and 8 mm thickness] with a hardness value about Rc 63. The mating surfaces of the pins and the disc were polished to a roughness of Ra = 0.1 μm before the start of the wear test. The wear tests were run under varying loads (10.0, 20.0, 30.0, 40.0, 50.0, 70.0 and 100 N) and varying sliding speeds (1.0, 2.0, 3.0 and 4.0 m/s) for a constant sliding distance (1,200 m). The measurement of the change in the specimen height due to wear during sliding and the coefficient of friction were measured continuously by electronic sensors. The LVDT used is capable of measuring a maximum displacement of ±2 mm with an accuracy of ±1 μm. A load cell is used to measure the frictional force. It has a maximum load capacity of 200 N and measures the frictional load at an accuracy of ±0.1 N in the load range 0–200 N. Frictional

Table 1 Test specimens and analyzed mechanical properties of Al–7Si and Al–7Si–2.5Cu cat alloys

Sl No	Alloy Design.	Alloy Composition	Addition level of GR (wt%)	Addition level of Modifier (wt%)	UTS (MPa)	Hardness (HB)
1	HP-1	Al–7Si	–	–	149	60
2	HP-2	Al–7Si–1M13	1.0	–	160	66
3	HP-3	Al–7Si–0.02Sr	–	0.02	168	70
4	HP-4	Al–7Si–2.5Cu	–	–	163	73
5	HP-5	Al–7Si–2.5Cu–1M13	1.0	–	184	85
6	HP-6	Al–7Si–2.5Cu–0.02Sr	–	0.02	194	90
7	HP-7	Al–7Si–2.5Cu–0.02Sr–1M13	1.0	0.02	200	98

GR: Grain refiner [M13 = Al–1Ti–3B] Modifier [Sr–Strontium]

Table 2 Chemical analysis of cast alloys and master alloys

Alloy	Composition (wt%)					
	Si	Fe	Sr	Ti	B	Al
Al	0.11	0.16	–	–	–	Balance
Al–7Si	6.98	0.17	–	–	–	Balance
Al–10Sr	0.12	0.17	10.0	–	–	Balance
Al–20Si	20.13	0.18	–	–	–	Balance
Al–1Ti–3B	0.16	0.17	–	1.13	2.25	Balance

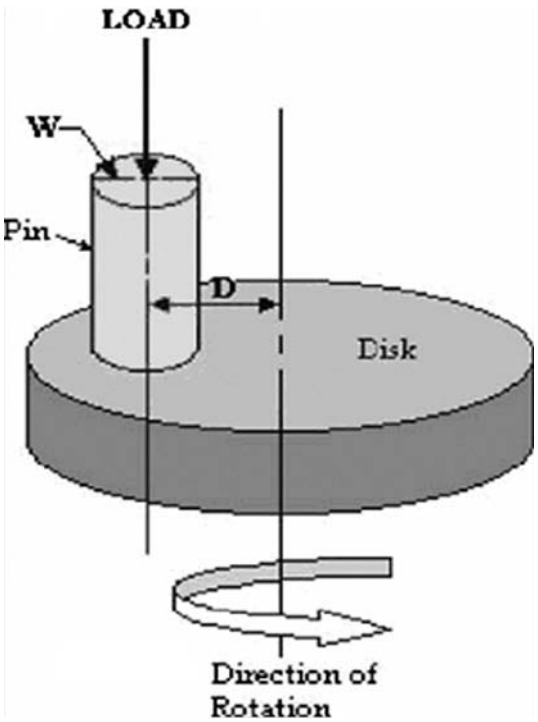

Fig. 1 Schematic diagram of Pin-On-Disc wear monitor

force (N) and pin length reduction (μm) were measured as a function of time. The volume loss and wear rates of the alloy specimens were calculated from the pin wear data. The wear test was carried out at a temperature of 25 °C and relative humidity of 45–50%. Before the tests, the polished pins were cleaned and degreased using ultrasonic cleaner, first with water and soap, followed with ethanol and finally with acetone. Cleaned samples were dried in an oven at 80 °C for 30 min. After each experiment the wear debris was collected for further examination. The wear debris and the tested pins were analyzed by X-ray diffraction (XRD), scanning electron microscope (SEM) to identify the mechanisms of wear. The Vickers hardness of the wearing surface of each pin was measured and recorded under a 5.0-Kg load after completion of each test.

Tensile testing of the specimens was carried out in Universal Testing Machine (AG-5000G, Shimadzu, Japan) in accordance with ASTM B-557-84 procedure.

Results

The microstructures of Al–7Si and Al–7Si–2.5Cu cast alloys treated by grain refiner and modifier

The microstructures of the Al–7Si and Al–7Si–2.5Cu cast alloys before and after grain refinement, modification and combined addition of both refiner and modifier are shown in Fig. 2a–g. It is observed that grain refinement; modification and combined addition of both refiner and modifier have profound influence on microstructures of the Al–7Si and Al–7Si–2.5Cu cast alloys. Figure 2a, d shows the microstructure of un treated alloys consisting of large

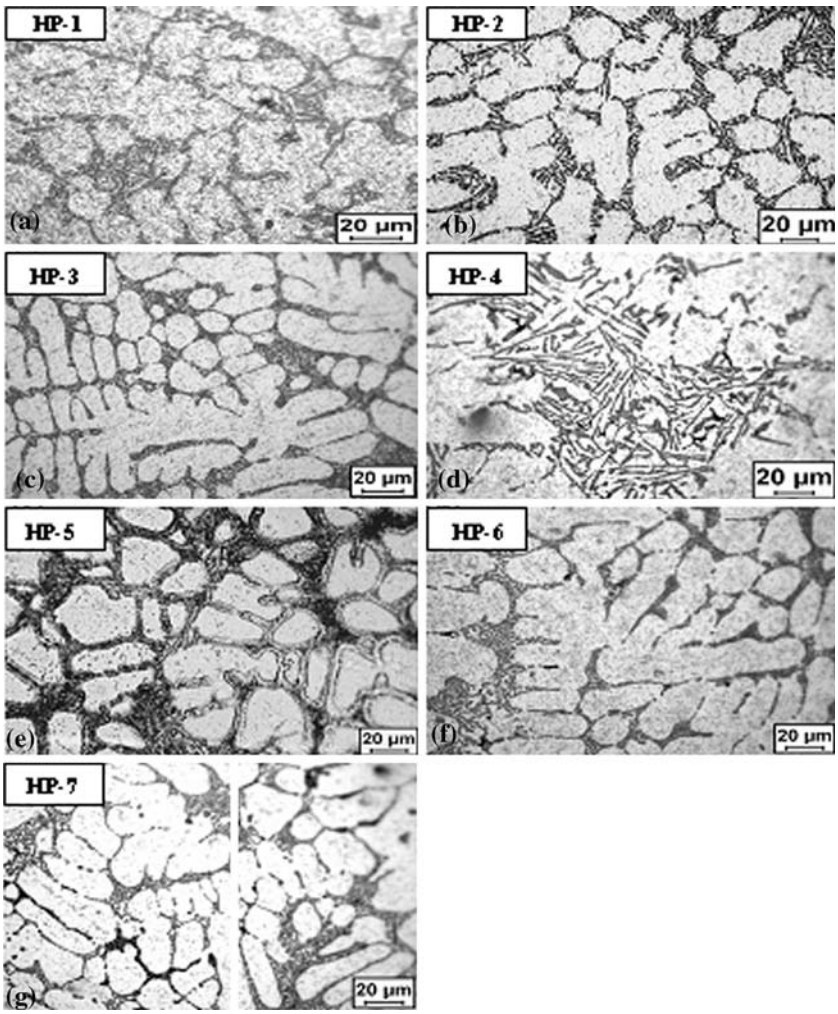

Fig. 2 Optical microphotographs of Al–7Si alloy (**a**) un-treated; (**b**) with grain refiner (1% of M13); (**c**) with modifier (0.02% Sr) and Al–7 Si–2.5 Cu alloy; (**d**) un-treated; (**e**) with grain refiner (1% of M13); (**f**) with modifier (0.02% Sr); and (**g**) with grain refiner (1% of M13) and modifier (0.02% Sr)

primary α-Al grains (soft phase), the plate like eutectic silicon and massive $CuAl_2$ particles in the interdendritic region. Figure 2b, e shows the microstructures of treated (1 wt% Al–1Ti–3B grain refiner) alloys consisting of fine equiaxed α-Al grains (soft phase), un modified eutectic and $CuAl_2$ particles in the interdendritic region. Figure 2c, f shows the microstructure of treated (0.02 wt% Sr modifier) alloy consisting of few primary α-Al grains (soft phase), uniformly distributed fine eutectic mixture and fine $CuAl_2$ particles in the interdendritic region. Figure 2g shows the microstructure treated by the combined addition of both grain refiner and modifier (1 wt% Al–1Ti–3B grain refiner and 0.02 wt% Sr modifier) alloy consisting of fine equiaxed α-Al grains (soft phase), uniformly distributed fine eutectic mixture and fine $CuAl_2$ particles in the interdendritic region.

The present experimental work confirms that, addition of grain refiner (1 wt% Al–1Ti–3B) to Al–7Si and Al–7Si–2.5Cu alloy significantly refines the coarse columnar primary α-Al grains to fine equiaxed α-Al grains due to the presence of AlB_2/TiB_2 particles present in the master alloy which are nucleating agents during the solidification of α-Al grains (soft phase), while the eutectic silicon particles appear to be unaffected as expected. Also the addition of modifier (0.02 wt% Sr) to Al–7Si and Al–7Si–2.5Cu alloy changes the plate like eutectic silicon to uniformly distributed fine particles (eutectic) and fine $CuAl_2$ particles in the interdendritic region [3]. The results also suggest that, the addition of Al–1Ti–3B master alloy along with Sr modifier to Al–7Si and Al–7Si–2.5Cu cast alloys shows more uniformly distributed α-Al grains, fine silicon and $CuAl_2$ particles in the interdendritic region compared to the individual addition of grain refiner or modifier. It is important to note that the alloys have been cast in a graphite mould surrounded by fireclay brick (slow cooling). Thus, further Improvement in the wear resistance and mechanical properties can be expected for fast cooled castings, as this can lead to further refinement of the microstructures.

Figure 3a shows the distribution of the intercept lengths Lα measured for the grains of soft phase for untreated Al–7Si–2.5Cu alloy. On the basis of measurements of the

longest length and shortest length, 15 classes were determined, with the width of a single class being 10 μm. From the data in the column chart, it is clear that the fraction of grains of solid phase Lα with the size up to 90–100 μm is as high as 80%. The microstructure also shows a few large primary coarser grains with intercept lengths between 130 and 150 μm. The size distribution of the measured intercept lengths for the eutectic constituent of the untreated Al–7Si–2.5Cu alloy is shown in Fig. 3b. In the size class up to 60–70 μm there are as many as 80% of the eutectic, which means that the eutectic of the untreated hypoeutectic alloy is coarse and plate like particles.

Figure 3c shows the distribution of the intercept lengths Lα measured for the grains of soft phase for grain refined (1 wt% Al–1Ti–3B) Al–7Si–2.5Cu alloy. The bandwidth of a single class is only 5 μm. In the size class up to 40–45 μm there are as many as 85% of all grains measured, which means that the soft phase of the hypoeutectic alloy is fine and equiaxed.

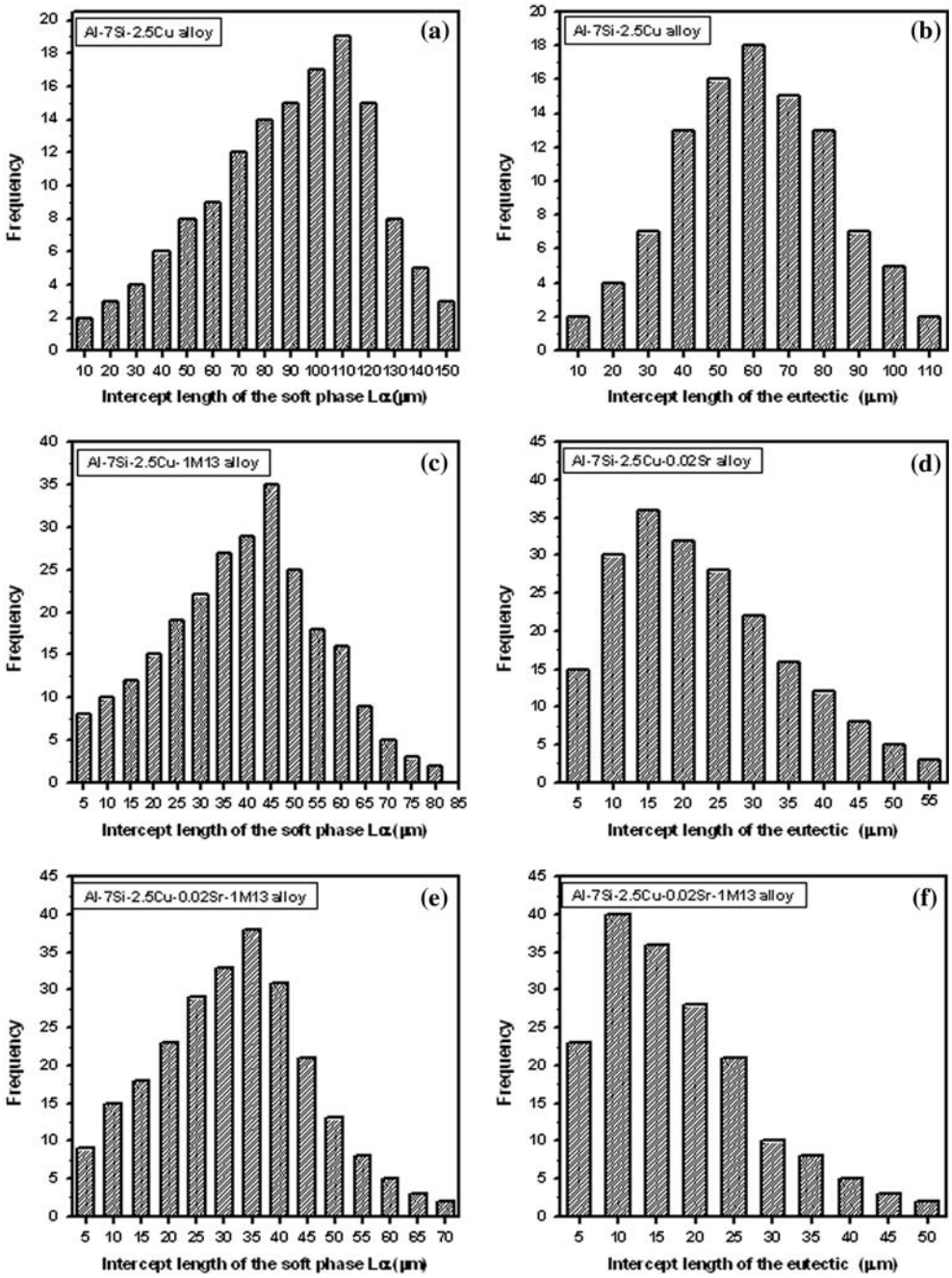

Fig. 3 Frequency of the intercept lengths of (**a**) Soft phase Lα and (**b**) Eutectic for the untreated hypoeutectic alloys; Frequency of the intercept lengths of (**c**) Soft phase Lα and (**d**) Eutectic for the treated hypoeutectic alloys; Frequency of the intercept lengths of (**e**) Soft phase Lα and (**f**) Eutectic for the combined treated hypoeutectic alloys

The size distribution of the measured intercept lengths for the eutectic of the modified (0.02 wt% Sr) Al–7Si–2.5Cu alloy is shown in Fig. 3d. In the size class up to 10–15 μm there are as many as 85% of all measured intercept lengths for the eutectic, which means that the eutectic of the treated hypoeutectic alloy is fine and uniformly distributed.

Figure 3e, f shows the distribution of Lα measured for the grains of soft phase and eutectic for the combined grain refined and modified (1 wt% Al–1Ti–3B and 0.02 wt% Sr) Al–7Si–2.5Cu alloy. It is clear that, the fraction of grains of soft phase Lα with the size up to 35–40 μm is as high as 80% and the fraction of eutectic with the size up to 10–15 μm is as high as 85%, which means that, the Fig. 3e, f clearly reveals fine equiaxed grains (soft phase) together with fine modified eutectic.

Effect of load on wear

When the load on the pin is increased, the actual area of contact would increase towards the nominal area, resulting in increased frictional force between two sliding surfaces. The increased frictional force and real surface area in contact will bring about higher wear. The influence of grain refinement and/or modification and combined addition of both on the sliding wear behavior of Al–7Si and Al–7Si–2.5Cu cast alloys under different loads (10.0, 20.0, 30.0, 40.0, 50.0, 70.0 and 100 N) with constant sliding speed (1.0 m/s) and constant sliding distance (1200 m) are shown in the Fig. 4a–d. It is noticeable from Fig. 4a–d that the volumes loss (mm^3), coefficient of friction (μ) and volumetric wear rate (mm^3/Nm) are more at higher loads for untreated samples. The wear test of the Al–7Si alloy, however, could not be carried out at the highest load of 100 N due to seizure. After a transient period, the wear loss was found to increase linearly with increasing load. However, Al–7Si–2.5Cu cast alloys containing grain refiner and/or modifier or combined addition of both show less volumes loss (mm^3), coefficient of friction (μ) and volumetric wear rate (mm^3/Nm) with increasing load. The hardness (VPN) of the worn surfaces was determined and the data are reported in the Table 3. This indicates that the hardness of the pin samples increased with increasing load.

SEM photographs of the worn surfaces of the pin samples (tested under 50-N load) are presented in Fig. 5. It is evident from Fig. 5a, d that the worn surfaces of the untreated Al–7Si and Al–7Si–2.5Cu alloys have undergone plastic flow and cracking. The worn surface of the untreated cast alloy, on the other hand, shows the presence of distinct grooves, suggesting ploughing of the pin surface. Figure 5b, c, e, f indicate plastic flow of the matrix, crack nucleation and propagation and crevice formation in the grain refined, modified and combined grain refined and modified Al–7Si–2.5Cu cast alloys. The morphology of the wear debris collected from the samples is shown in Fig. 6. The un-treated alloy may undergo more oxidation during the wear test due to higher temperature.

Effect of various sliding speeds on wear

The influence of grain refinement and/or modification and combined addition on the sliding wear behavior of Al–7Si and Al–7Si–2.5Cu cast alloys under various sliding speeds (1.0, 2.0, 3.0 and 4.0 m/s) with constant load (50 N) and constant sliding distance (1200 m) are shown in the Fig. 7a–d. It is noticeable from Fig 7a–d, the volume loss, and coefficient of friction and wears rate decreases with increasing sliding speed in all the specimens of Al–7Si and Al–7Si–2.5Cu cast alloys. However less volume loss, coefficient of friction and wear rates were observed in case of the grain refined and/or modified Al–7Si–2.5Cu cast alloys.

Reduction in volume loss, coefficient of friction and wear rates seen with the increase in sliding speed (Fig. 7a–d) is possibly due to increased contamination of sliding interface by decreased oxide layer breakup in less contact time. The presence of oxide layer reduces the chance of direct metallic contact and therefore asperities interaction is reduced, which is a prerequisite for adhesive wear. Moreover, increasing the sliding speed also increases the interface temperature. Rise in temperature with in limit increases the ability of soft aluminum matrix to accommodate hard and brittle second phase silicon particles. High seizure resistance of combined grain refined and modified Al–7Si–2.5Cu cast alloy may possibly due to the presence of comparatively more thermally stable inter-metallic compound of alloys of copper, which resist the thermal softening particularly at high speed and contact load.

Discussion

The combined grain refined and modified Al–7Si–2.5Cu cast alloy offered the best wear resistance at the higher loads (Fig. 4d). The wear resistance of the un-treated Al–7Si alloy was distinctly inferior to the experimental alloy. In fact, wear testing could not be conducted on the un-treated Al–7Si alloy pin sample at 100 N (highest load in the present work) due to the occurrence of seizure. This can be explained by the mechanism proposed by Lim and Ashby [15]. When the pin surfaces are placed in contact with the disc, the real area of pin contact is usually very small. The large local pressure at the points of real contact (the asperity contacts) can forge soft metallic junctions between the surfaces even under static conditions. Under large-enough loads, the real area of contact grows until it is

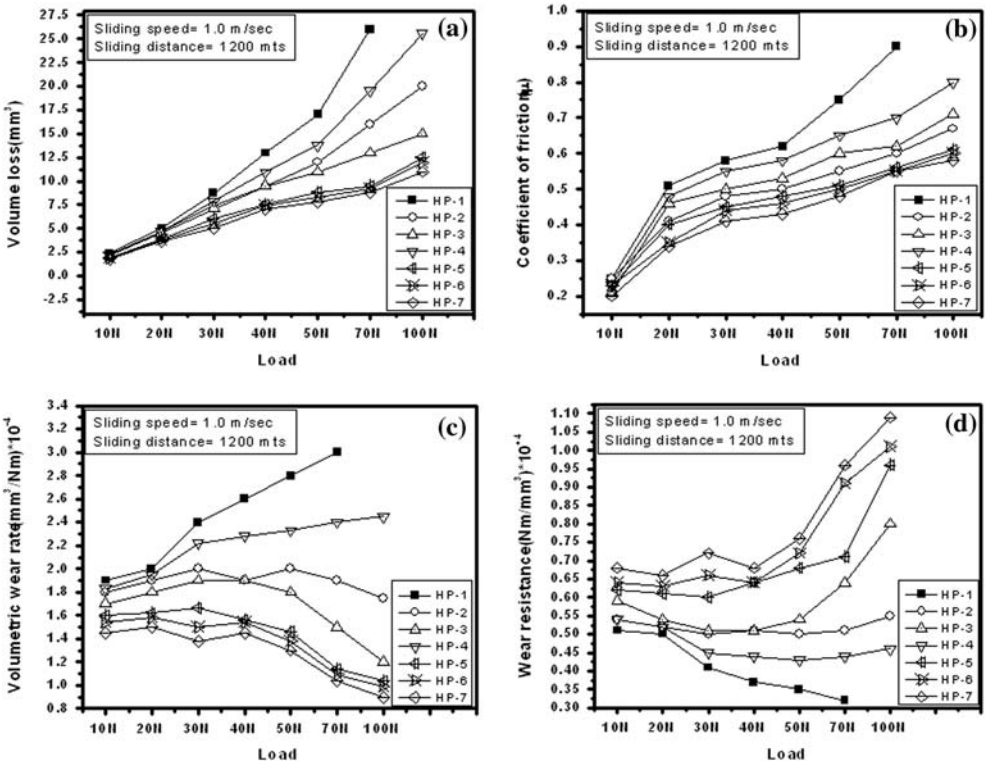

Fig. 4 (**a**) Variation of volume loss versus different loads at constant Sliding Speed (1 m/s) and constant Sliding distance (1200 m); (**b**) Variation of coefficient of friction versus different loads at constant sliding speed (1.0 m/s) and constant sliding distance (1200 m); (**c**) Variation of volumetric wear rate versus different loads at constant sliding speed (1.0 m/s) and constant sliding distance (1200 m). (**d**) Variation of wear resistance versus different loads at constant sliding speed (1.0 m/s) and constant sliding distance (1200 m)

Table 3 Hardness (VPN) of as cast and worn samples (Load: 5.0 Kg)

SI No	Alloy	Hardness (VPN)					
		As cast	20N	30N	50N	70N	100N
1	HP-1	32	40	46	50	–	–
2	HP-2	37	46	59	76	89	98
3	HP-3	43	55	71	92	105	128
4	HP-4	46	59	66	78	86	–
5	HP-5	60	70	88	103	126	141
6	HP-6	61	75	86	107	128	149
7	HP-7	68	80	92	115	138	161

equal to the nominal area of the pin surfaces and the surface seizes completely. The microstructure of Al–7Si alloy consists of large elongated primary α-Al grains and the eutectic silicon (plate like) induces poor ductility to the casting. Unmodified acicular silicon structure acts as internal stress risers in the microstructure and provides easy path for fracture. The large elongated primary α-Al grains and plate like silicon particles in the unmodified Al–7Si alloy is usually considered undesirable from toughness and ductility points of view. It is interesting that such non-uniform distribution of primary α-Al grains and hard silicon particles does not improve the wear resistance either. The wear resistance of the un-treated alloys decreased continuously with increasing wear load (Fig. 3d). Better wear resistance should be achieved through fine equiaxed primary α-Al grains and uniform distribution of the second phase particles. In this context, the performance of different grain refiners and modifier on Al–7Si and Al–7Si–2.5Cu cast alloys were tested. The combined grain refined and modified Al–7Si–2.5Cu cast alloy recorded higher wear resistance at the highest load (HP-7). It is, thus, obvious that, the addition of grain refiner (Al–1Ti–3B) and modifier (Sr) converts large α-Al grains into fine equiaxed α-Al grains, eutectic silicon (plate like) into fine particles and fine $CuAl_2$ particles in the interdendritic region support the wear load better than elongated α-Al grains, non-uniformly distributed plate like silicon and massive $CuAl_2$ particles. Crack nucleation generally occurs at some depth below the surface rather than very near the surface, owing to the very high hydrostatic compressive pressure acting near the asperity contact [16]. Thus, once a crack is nucleated, its propagation is slow and seizure does not

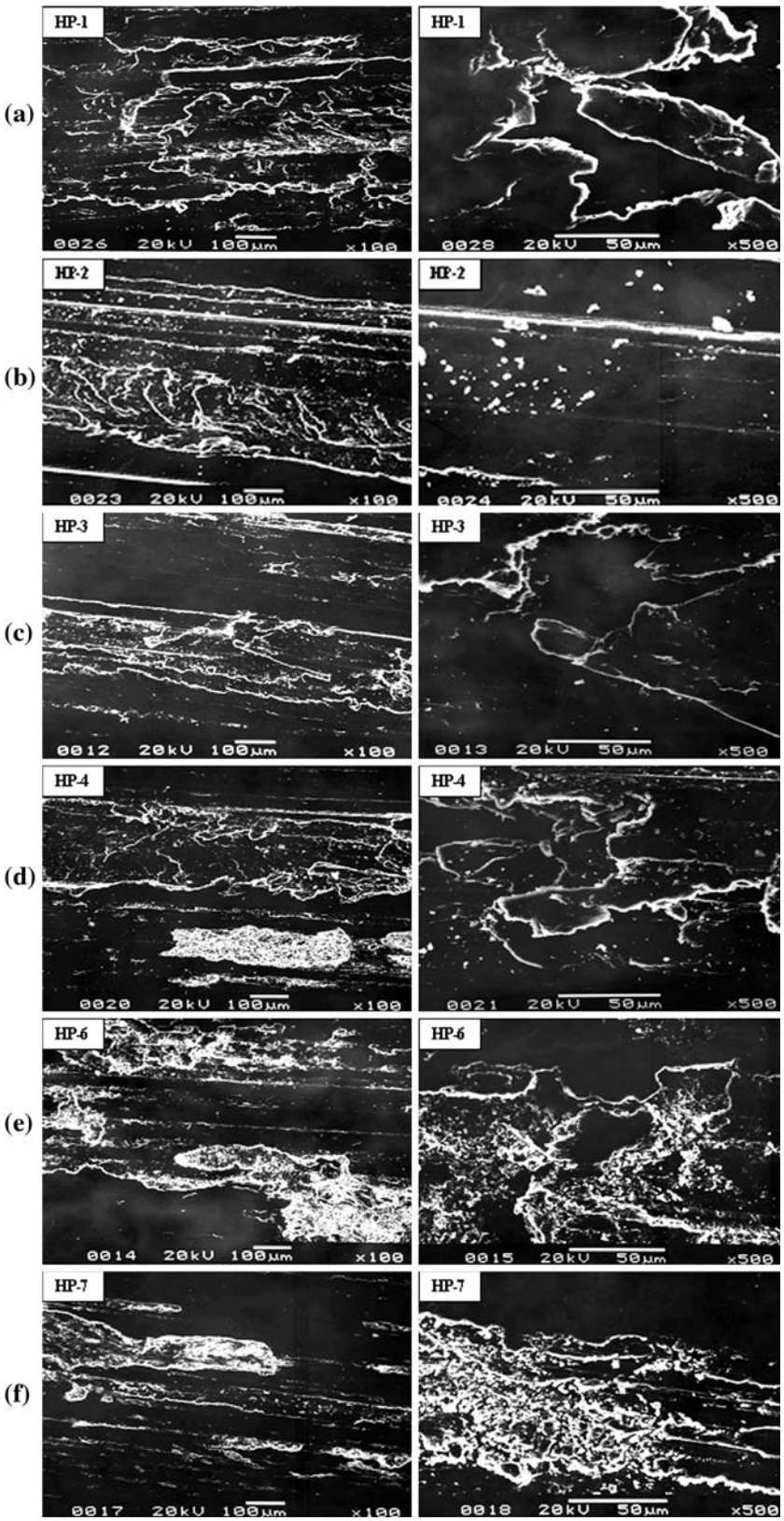

Fig. 5 SEM photographs (Low and High Magnification) of worn surfaces of hypoeutectic Al–Si alloys

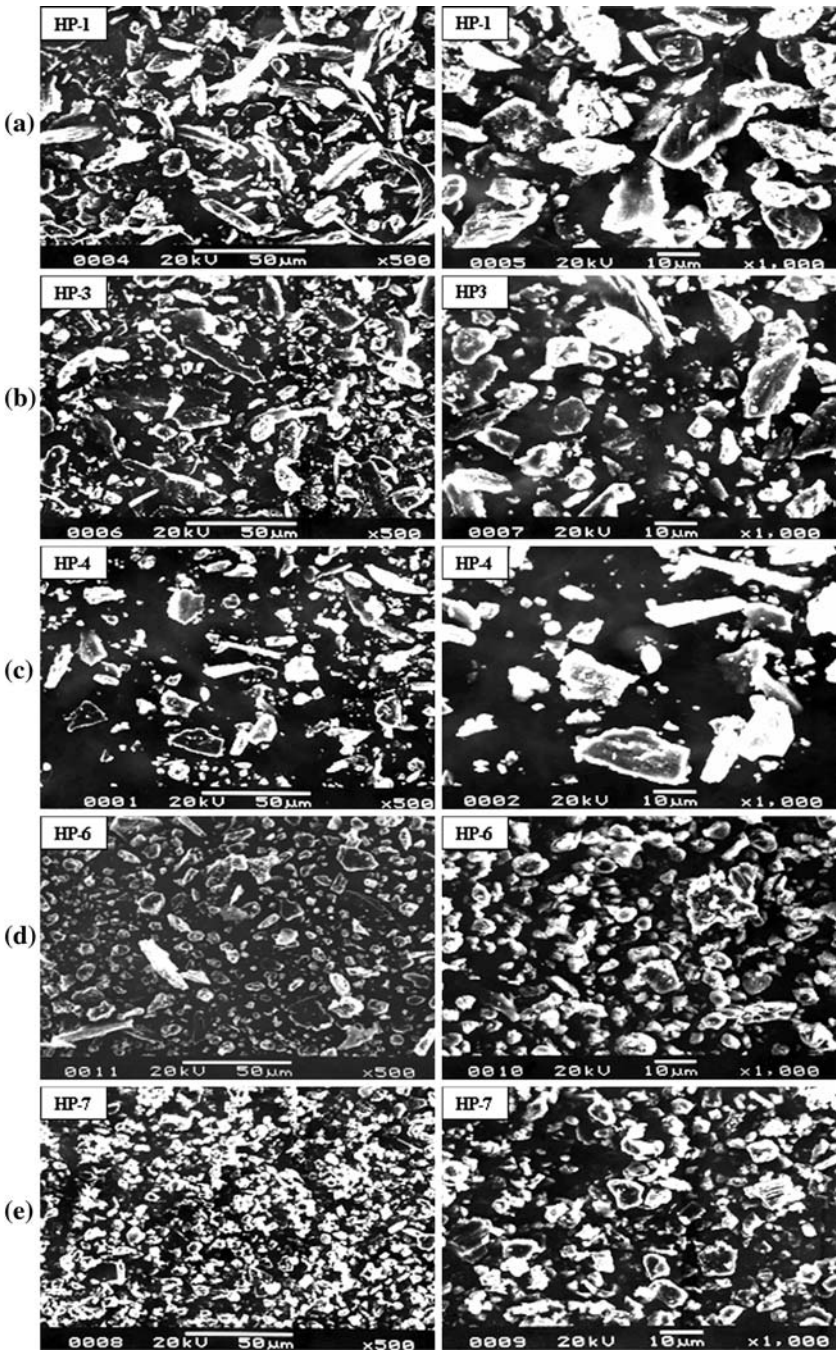

Fig. 6 SEM photographs (Low and High Magnification) of wear debris of hypoeutectic Al–Si alloys

occur, owing to the presence of well-distributed particles in the matrix [17] even at a high load of 100 N. In the Al–7Si alloy, the presence of Si particles alone is not adequate for such high-wear load.

Increasing test loads lead to greater plastic deformation and wear. Increased work hardening in specimens tested at higher loads is evident from the data on hardness of the worn specimen presented in Table 3. But the trends in wear curves (Fig. 4a) show that the steady state stage was not reached during the testing times for these alloys and loads. However, the overall wear resistance increased due to appreciable work hardening of the alloys with grain refinement and modification. On the contrary, the wear resistance of the un-treated Al–7Si alloy (alloy HP-1; Fig. 4d) continued to decrease with increasing load. The extent of work hardening here was small.

In order to investigate the wear mechanism, the surfaces of the worn samples were examined under SEM. The low magnification SEM photographs (Fig. 5) show fine scoring marks. The worn surface of the Al–7Si alloy at 50-N load

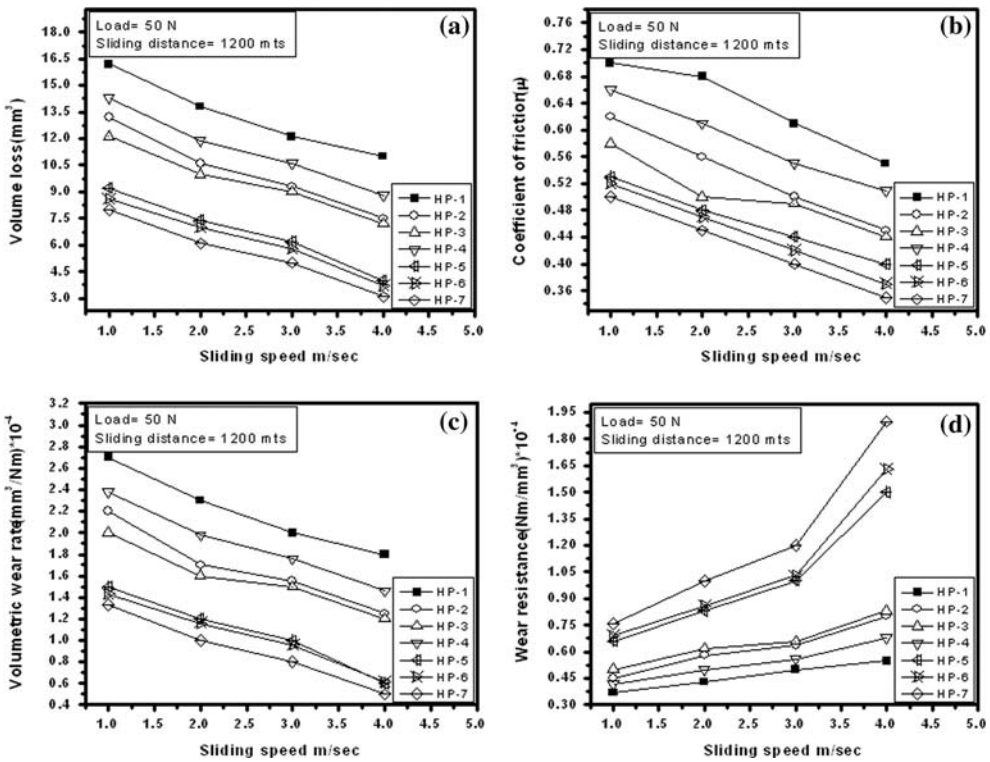

Fig. 7 (**a**) Variation of volume loss versus sliding speeds at constant load (50 N) and constant sliding distance (1200 m); (**b**) Variation of coefficient of friction versus sliding speeds at constant load (50 N) and Constant sliding distance (1200 m); (**c**) Variation of volumetric wear rate versus sliding speeds at constant load (50 N) and constant sliding distance (1200 m); (**d**) Variation of wear resistance versus sliding speeds at constant load (50 N) and constant sliding distance (1200 m)

was more heavily cracked than those of grain refined and modified Al–7Si–2.5Cu cast alloys. The scoring may be due to abrasion by entrapped debris, work-hardened deposits on the counter face or hard asperities on the hardened steel counter face [18].

On examination of the worn surfaces at higher magnification, evidence of extensive plastic flow and cracking was observed. These are the two likely modes of crack initiation and propagation. Cracks may initiate in the highly work-hardened layer, particularly in the subsurface region. When cracks grow and get interconnected, a layer of metal is removed. This is delamination wear [16]. Fig. 5a, d suggest such a mechanism. The SEM photographs (Fig. 6a, c) indicate that the particles in the wear debris were mainly sheet-like. This is an indication of delamination wear. It is also possible that the hard dispersoid particles or fractured pieces thereof are mechanically dislodged during wear. The pinholes so formed act as potential sites for nucleation and growth of cracks, paving the way for delamination wear (Fig. 5a, d). The dispersoid particles in the Al–7Si–2.5Cu cast alloys may act as asperities, which continue to support the load until they are fractured and leveled off. It appears from Table 3 that the extent of work hardening increases with increasing degree of grain refinement and modification. This suggests that grain refined and modified alloys with finer dispersoid particles undergo greater plastic deformation (Figs. 5e, f). The delaminated wear debris particles are already so severely work-hardened and fractured that they do not stick to the sliding surface any further and are removed. The high magnification SEM picture of the wear debris in Fig. 5f confirms this fact. The worn surface and the wear debris of the un-treated Al–7Si alloy appear to be oxidized, particularly at the highest load (Fig. 6a).

The coefficient of friction attained a value range (allowing for the scatter in the data) after an initial transient period, as indicated in Fig. 4 (b). The coefficient of friction increases uniformly with increasing load in most of the cases. The coefficient of friction in the case of the grain refined and a modified Al–7Si–2.5Cu cast alloy was lower at all the loads as shown in Fig. 4b. The sudden increases in the friction coefficient at 70-N load for un treated alloy indicate adhesion of the pin to sliding surface. Such adhesion was conspicuous by is absence in the case of the Al–7Si alloy, which suffered seizure at 70-N load. At this load, the frictional heat generated is sufficient to cause localized heating, resulting in sticking of the pin to the disc. The rise in the coefficient of friction with the increase in wear load may be attributed to (a) enhanced accumulation of the wear debris consisting of large volume fraction of hard aluminide and silicide particles pulled out of the matrix during wear at the pin and disc interface and (b) oxidation of the wearing surface. The deep furrows on the pin surfaces may also be accounted for by the cutting action of the hard particles of aluminide and silicide having hardness of 650–850 VPN. Fortunately, a simultaneous

work hardening of the matrix by plastic deformation helped in reducing the extent of wear of the samples at high loads. During wear at high loads, the temperature increases appreciably lowering the strength of the materials in contact resulting in increased contact area and coefficient of friction. The stronger grain refined and modified alloys recorded the lowest coefficient of friction.

Reduction in volume loss, coefficient of friction and wear rates with the increase in sliding speed (Fig. 7a–d) is possibly due to increased contamination of sliding interface by oxide layer. The presence of oxide layer reduces the chance of direct metallic contact and therefore asperities interaction is reduces, which is a prerequisite for adhesive wear [19]. Moreover, increasing the sliding speed also increases the interface temperature. Rise in temperature within limit increases the ability of soft aluminum matrix to accommodate hard and brittle second phase silicon particles [20]. If temperature goes beyond certain critical value, thermal softening of the material in sub-surface region takes place, which leads to large-scale plastic deformation during the sliding under external load [21]. Under such conditions metallic wear takes place. Increased solid solution strengthening, inter-metallic compound and precipitation hardening in the presence of alloying elements may be attributed to comparatively better wear resistance and hardness of combined grain refined and modified Al–7Si–2.5Cu cast alloys than un-treated Al–7Si alloy. High seizure resistance of combined grain refined and modified Al–7Si–2.5Cu cast alloy may possibly due to the presence of comparatively more thermally stable inter-metallic compound of alloys of copper, which resist the thermal softening particularly at high speed and contact load. At high sliding speed, resulting high interface temperature may increase the back transfer of Fe, which may diffuse into the near sliding surface material and change the composition. X-ray diffraction (XRD) and EDAX analysis of wear debris (Fig. 8a–b) clearly show the presence of Fe_2O_3, Fe, Al and Si. The Diffusion of Fe into the alloy may cause precipitation/dispersion hardening by reacting with different alloying elements. Opportunities to form such hard inter-metallic compound will be less in un-treated Al–7Si alloy because of the absence of other alloying elements [21]. Dispersion hardening in the presence of alloying element may be a possible reason for higher seizure resistance of combined grain refined and modified Al–7Si–2.5 Cu alloy than un-treated Al–7Si alloy. A D Sarkar has reported that friction depends also on material properties such as hardness, strain, density, shear strength, modulus of elasticity and ultimate tensile strength [10]. High hardness of the combined grain refined and modified Al–7Si–2.5Cu cast alloy than un-treated Al–7Si alloy (Table 1) may also reduce the incidence of fracture and deformation of surface asperities and therefore real

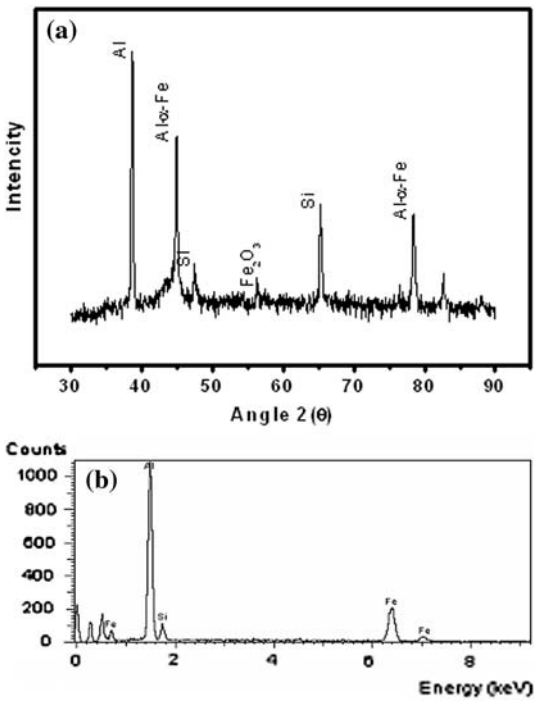

Fig. 8 (**a**) X-ray diffraction pattern of wear debris; (**b**) EDAX pattern of wear debris

contact area may reduce. Hence, the above may be attributed to low coefficient of friction in sliding of combined grain refined and modified Al–7Si–2.5Cu cast alloy than that for un-treated Al–7Si alloy under similar condition. Friction force arises from two main factors: (a) force required to shear minute welds formed at contact points between two rubbing surfaces and (b) force required to blow the hard asperities over a soft surface. Therefore, higher frictional force in sliding of un-treated Al–7Si alloy than that of combined grain refined and modified Al–7Si–2.5Cu cast alloy may be attributed to low hardness and strength of un-treated Al–7Si alloy due to the absence of alloying elements. At low sliding speeds, longer time is available for formation and growth of junction asperity contact regions, which increases the force required to shear off the junction to maintain the relative motion; therefore it justifies the high friction coefficient at low sliding speed as compared to that at high sliding speed.

Conclusions

The influence of melt treatments on the wear behavior of the Al-7Si and Al-7Si-2.5Cu cast alloys was investigated and the following conclusions could be drawn:

1. The measurements performed confirmed that the wear behavior is mainly influenced by the sizes of the soft phase and eutectic constituents in the alloys.

2. The Al-Si alloys investigated exhibit plastic deformation and work hardening during wear testing; the grain refined and modified Al-7Si-2.5Cu cast alloys work-hardened to a greater extent than the un-treated alloys.
3. The wear resistance decreases with increasing load in case of untreated alloys. In the grain refined and modified alloys, it increases with increasing load due to higher work hardening rates.
4. Wear occurs by plastic deformation and cracking of the matrix followed by delamination of flakes. In addition, detached hard despersoid particles also contribute to wear.
5. Coefficient of friction and temperature rise sharply at high- wear load
6. Combined grain refinement and modification minimizes oxidation of the matrix. The best-combined grain refined and modified (Al-1Ti-3B + Sr) alloys recorded minimum coefficient of friction and temperature at high-wear load.
7. Reduction in volume loss, coefficient of friction and wear rates with the increase in sliding speed is possibly due to

(a) Increased contamination of sliding interface by oxide layer.
(b) Increased solid solution strengthening, inter-metallic compound and precipitation hardening in the presence of alloying elements may be attributed to comparatively better wear resistance.

References

1. Okabayashi K, Kawamoto M (1968) Bull Uni Osaka Prefecture A 17
2. Rohatgi PK, Pai BC (1974) Wear 28:353
3. Torabian H, Pathak JP, Tiwari SN (1994) Wear 172:49
4. Clarke J, Sarkar AD (1979) Wear 54:7
5. Balu PJ (1981) Wear 71(1):29
6. Shivnath R, Sengupta PK, Eyre TS (1977) British Foundry Jl 70(12):349
7. Pramila Bai BN, Biswas SK (1984) J Mater Sci 19:3588
8. Pramila Bai BN, Biswas SK (1987) Wear 120:61
9. Pramila Bai BN, Biswas SK, Kumtekar NN (1983) Wear 87:237
10. Sarkar AD (1975) Wear 31:331
11. Somi Redy A, Premila Bai BN, Murthy KSS, Biswas SK (1994) Wear 171:117
12. Eyre TS (1980) Microstruct Sci 8:141
13. Kori SA, Murty BS, Chakraborty M (2000) Mater Sci Engg A283:98
14. Massalksi TB (1990) In: Scott WW Jr (ed) Binary alloy Phase Diagrams, 2nd edn. America, p 540
15. Lim SC, Ashby MS (1987) Act Metall 35(1):1
16. Jahanmir S, Suh NP (1977) wear 44:17
17. Yang CC, Hsu WM, Chang E (1997) Mater Sci Tech 13:687
18. Pramila Bai BN, Biswas SK (1991) Scr Metall Mater 39:833
19. Lingaurd S, Fu KH, Chueng KH (1979) Wear 759
20. Razavizadeh K, Eyre TS (1982) Wear 79:325
21. Madakson Peter B (1983) Wear 94:193